SOUND GENERATION AND INTERACTIONS OF SHOCK WAVES WITH ROWS OF VORTICES

Xu Dongyang(许东洋)[1,2], *Guan Hui*(关晖)[3], *Wu Chuijie*(吴锤结)[1,2]

(1. State Key Laboratory of Structural Analysis for Industrial Equipment, Dalian University of Technology, Dalian, 116024, P. R. China;
2. School of Aeronautics and Astronautics, Dalian University of Technology, Dalian, 116024, P. R. China;
3. Department of Mathematics & Physics, PLA University of Science and Technology, Nanjing, 211101, P. R. China)

Abstract: Interactions of shock waves and rows of vortices are studied by solving the two-dimensional, compressible Euler equations with a fifth-order weighted essentially non-oscillatory finite difference scheme. For a compressible flow the Mach number of the shock wave and vortex equals to 1.05 and 0.25, respectively. The resulting flow field contains complex shock structures, such as multiple shock focusing and reflecting regions. At the meantime, sound waves are generated, interrupted and reformed when they touch the main and reflected shock waves.

Key words: shock wave; vortex street composed of four vortices; interaction; sound wave

CLC number: O353.1 **Document code**: A **Article ID**: 1005-1120(2013)03-0276-06

INTRODUCTION

The nonlinear interaction between the shock waves and vortices leads to shock deformation, local compression and flow field expansion, and forming acoustic waves. It is one of the major sources of aerodynamic noise. The vortices are the basic elements of supersonic turbulence. The interaction between shock waves and vortices can be regarded as a simple model for shock turbulence interaction which is one of the most complicated phenomena in supersonic flow. The interactions between a shock wave and a single vortex, a vortex pair have been extensively studied.

Inoue, et al[1] observed different cases of interaction while simulating interaction between a shock wave and a vortex pair of two types. A brief summary of a shock-single vortex and vortex pair interaction is given in Refs. [2-3] by showing three sound generation mechanisms. Our purpose is to study the details of sound generation mechanisms where a shock wave is interacting with a vortex street composed of four vortices which can be seen as a simple model of wave vortex.

1 MATHEMATICAL FORMULATION AND NUMERICAL PROCEDURE

1.1 Physical model

Fig. 1 is the schematic diagram of the flow model. The computational domain is prescribed to be a two dimentional rectangular in x-y plan ($-30 \leqslant x \leqslant 20$, $-25 \leqslant y \leqslant 25$). The incident

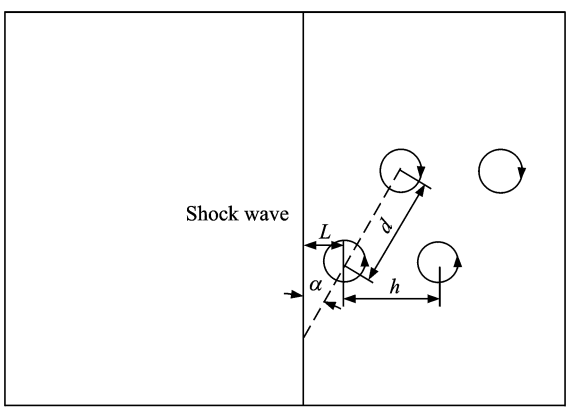

Fig. 1 Schematic diagram of flow model

Foundation item: Supported by the National Natural Science Foundation of China (11072053).

Received date: 2013-04-27; **revision received date**: 2013-07-07

Corresponding author: Wu Chuijie, Professor, E-mail: cjwudut@dlut.edu.cn.

shock wave is set to be stationary at $x=0$ in the computation. The vortex street moves toward the shock from the right to the left at a speed of v_s. The Mach number of the shock and the vortex is prescribed to be 1.05 and 0.25, respectively. The initial flow field is produced by each single vortex. At the initial time the initial distances d and L are set to be 4.0, the initial angle α is 45°, and h is the distance between two vortices.

1.2 WENO scheme

The numerical method for this computation is the fifth-order weighted essentially non-oscillatory (WENO) finite difference scheme developed by Shu[4] which is to solve the two-dimensional unsteady compressible Euler equations. The basic idea is as follows: A convex combination of all of candidates stencils are used to form the reconstruction instead of only one. To be more specific, suppose k candidate stencils

$$S_r(i)=\{x_{i-r},\cdots,x_{i-r+k-1}\}\quad r=0,\cdots,k-1 \tag{1}$$

Produce k different reconstructions to the value $v_{i+\frac{1}{2}}$

$$v_{i+\frac{1}{2}}^{(r)}=\sum_{j=0}^{k-1}c_{rj}\bar{v}_{i-r+j}\quad r=0,\cdots,k-1 \tag{2}$$

WENO reconstructions takes a convex combination of all $v_{i+\frac{1}{2}}^{(r)}$ as a new approximation to the cell boundary value $v(x_{i+\frac{1}{2}})$

$$v_{i+\frac{1}{2}}=\sum_{r=0}^{k-1}\omega^{(r)}v_{i+\frac{1}{2}} \tag{3}$$

For stability and consistency, we require

$$\sum_{r=0}^{k-1}\omega_r=1\quad \omega_r\geqslant 0 \tag{4}$$

If function $v(x)$ is smooth in all of the candidate stencils, there are constants d_r such that

$$v_{i+\frac{1}{2}}=\sum_{r=0}^{k-1}d_r v_{i+\frac{1}{2}}^{(r)}=v(x_{i+\frac{1}{2}})+O(\Delta x^{2k-1}) \tag{5}$$

We can see that d_r is always positive and, due to consistency, $\sum_{r=0}^{k-1}d_r=1$.

In this smooth case, here is

$$\omega_r=d_r+O(\Delta x^{k-1})\quad r=0,\cdots,k-1 \tag{6}$$

Eq. (6) implies $(2k-1)$-th-order accuracy

$$v_{i+\frac{1}{2}}=\sum_{r=0}^{k-1}\omega_r v_{i+\frac{1}{2}}^{(r)}=v(x_{i+\frac{1}{2}})+O(\Delta x^{2k-1}) \tag{7}$$

Because

$$\sum_{r=0}^{k-1}\omega_r v_{i+\frac{1}{2}}^{(r)}-\sum_{r=0}^{k-1}d_r v_{i+\frac{1}{2}}^{(r)}=\sum_{r=0}^{k-1}(\omega_r-d_r)(v_{i+\frac{1}{2}}^{(r)}-v(x_{i+\frac{1}{2}}))=\sum_{r=0}^{k-1}O(\Delta x^{k-1})O(\Delta x^{2k-1}) \tag{8}$$

When function $v(x)$ has a discontinuity in one or more of the stencils, the corresponding ω_r will essentially be 0. For computational efficiency, the following form of weights is used

$$\omega_r=\frac{\alpha_r}{\sum_{s=0}^{k-1}\alpha_s}\quad r=0,\cdots,k-1 \tag{9}$$

where

$$\alpha_r=\frac{d_r}{(\varepsilon+\beta_r)^2}$$

Let the reconstruction polynomial on the stencils be denoted by $p_r(x)$, the following form of β_r is chosen

$$\beta_r=\sum_{l=1}^{k-1}\int_{x_{i-\frac{1}{2}}}^{x_{i+\frac{1}{2}}}\Delta x^{2l-1}\left(\frac{\partial^l p_r(x)}{\partial^l x}\right)^2\mathrm{d}x \tag{10}$$

For $k=3$, here is

$$\beta_0=\frac{13}{12}(\bar{v}_i-2\bar{v}_{i+1}+\bar{v}_{i+2})^2+\frac{1}{4}(3\bar{v}_i-4\bar{v}_{i+1}+\bar{v}_{i+2})^2$$

$$\beta_1=\frac{13}{12}(\bar{v}_{i-1}-2\bar{v}_i+\bar{v}_{i+1})^2+\frac{1}{4}(\bar{v}_{i-1}-\bar{v}_{i+1})^2$$

$$\beta_2=\frac{13}{12}(\bar{v}_{-2i}-2\bar{v}_{i-1}+\bar{v}_i)^2+\frac{1}{4}(\bar{v}_{i-2}-4\bar{v}_{i-1}+3\bar{v}_i)^2$$

This provides a fifth-order WENO scheme. It has fifth-order accuracy in smooth regions and third-order accuracy in discontinuous regions with the solution essentially non-oscillatory and sharp shock transitions near discontinuities.

2 NUMERICAL RESULTS AND DISCUSSION

2.1 Shock structure

The interaction between a shock wave and a vortex street is more complicated than that between a shock wave and a vortex pair. The shock dynamics is strongly affected by the condition of the vortex in the process of shock vortex interaction, while the shock structure acts differently for the vortex pair and rows of vortices.

In Fig. 2, R shows the reflected shock wave

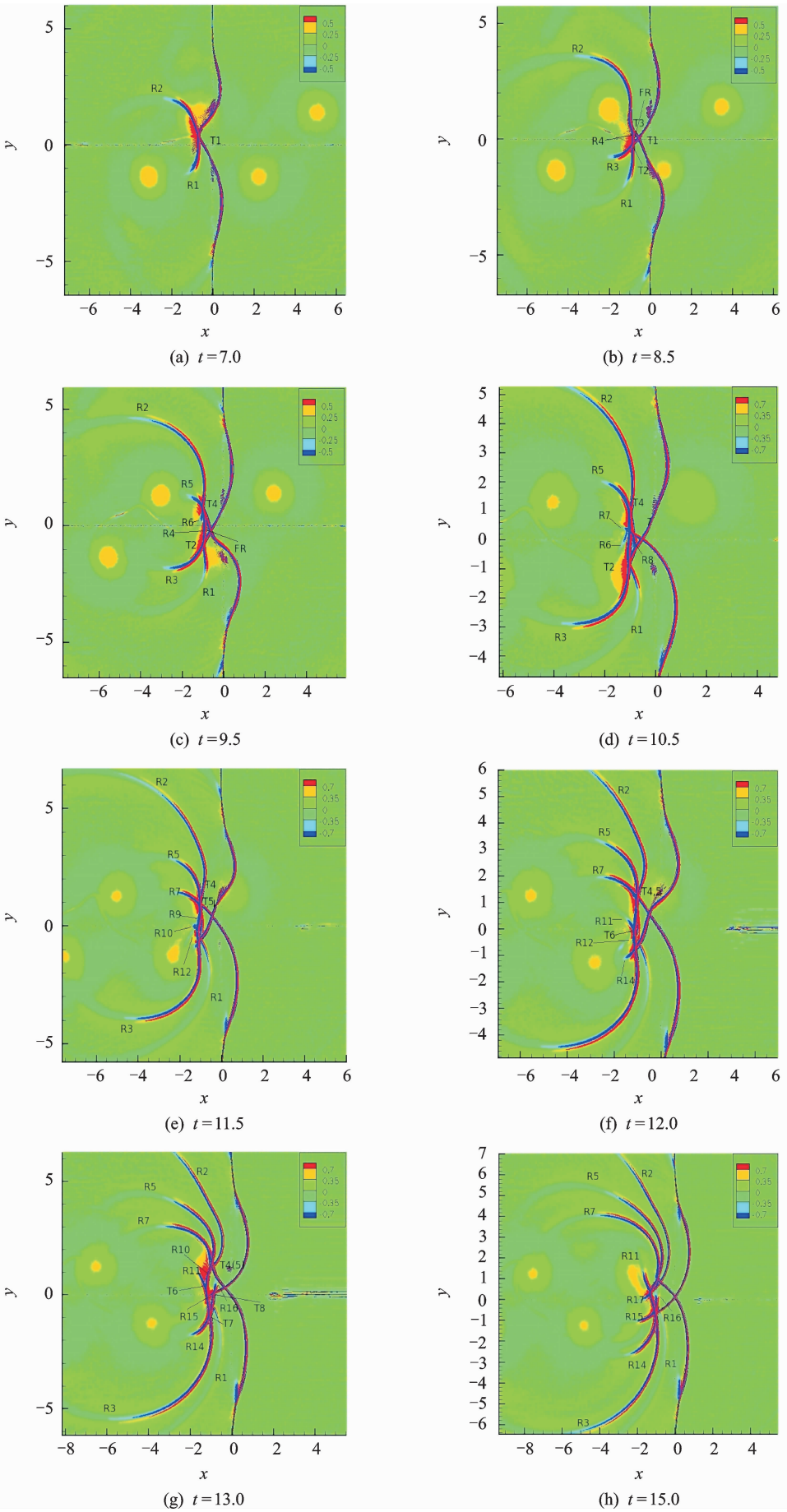

Fig. 2 Evolution of shock structure of shock and vortex street interaction

T the triple point, and t the time. Fig. 2 is the evolution of the flow field of interaction between the shock wave and a vortex street composed of four vortices. When the shock wave interacts with the first two vortices, it is much like the case of shock-vortex pair interaction. While the distorted shock touches the third vortex, the interaction is different to some extent. The vortices interact with shock focusing regions as well as the reflected shock waves. A single reflected shock wave is not strong, but when several reflected shock waves fold and merge together, it will be strong enough to be able to interact with the rear vortices. The vortex Mach number $Ma_v = 0.25$ is not strong, but the resulting field contains complex shock structures such as shock focusing, folding, and crossing. The shock focusing region and multiple shock focusing region stay for a longer period of time.

2.2 Trajectory of triple points

The trajectory of the triple point $T1$, $T8$ is recorded to further showing the feature of the resulting field. The point almost exits in the whole process of interactions and there is an oscillatory movement around the horizontal line, $y = 0$, which agrees with the trend of the vortex interacting with the shock (Fig. 3). The moving track of triple point $T8$ illustrates the process that multiple reflected shock waves fold, merge and form a new stronger shock wave (Fig. 4). Here we can see Figs. 2(g—h) for reference.

2.3 Evolution and mechanism of sound generation

The generation and propagation of sound waves is one of the most interesting phenomena in the problem of shock vortex interaction. Because of the complexities of the vortex street, the interaction among vortices and multiple reflected shock-sound interaction, the sound wave generation are not regular and symmetrical. Fig. 5 is the evolution of the sound wave generated in the interaction of a shock of $Ma_s = 1.05$ and rows of vortices of $Ma_v = 0.25$. In this figure, the solid lines represent the compression ($\Delta p > 0$), while the dashed lines represent the rarefaction region ($\Delta p < 0$).

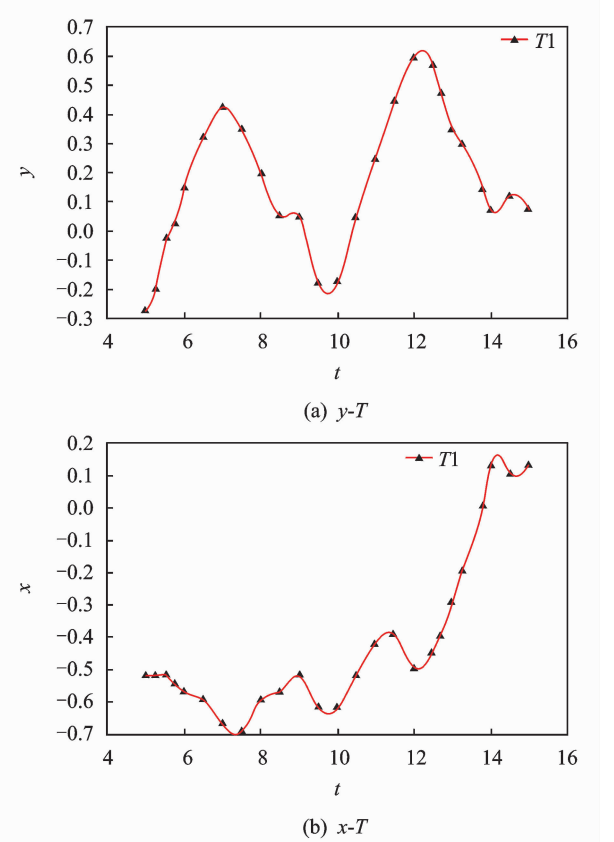

Fig. 3 Trajectory of triple point $T1$

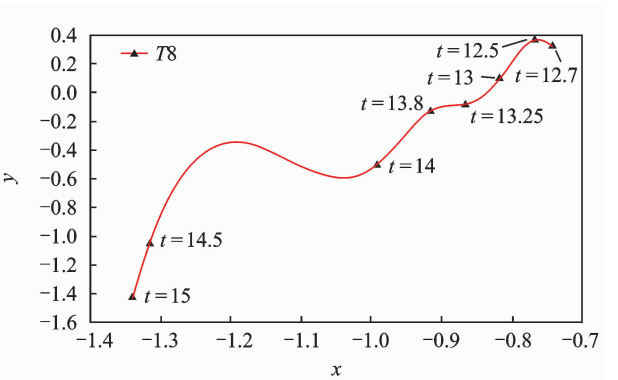

Fig. 4 Trajectory of triple point $T8$

As seen from Fig. 5, there are three features in the interaction of a shock wave and rows of vortices. (1) The vortex coupling effect is significant. The vortex dipoles of vortex coupling develope in the whole process of the interaction. (2) The interaction can be regarded as between a shock wave, vortices and smaller scale vortices (Fig. 5(c)). (3) The vortices are not strong, but the sound waves are broken down by reflected shock waves which become more and stronger, and the sound waves generated earlier, the sound

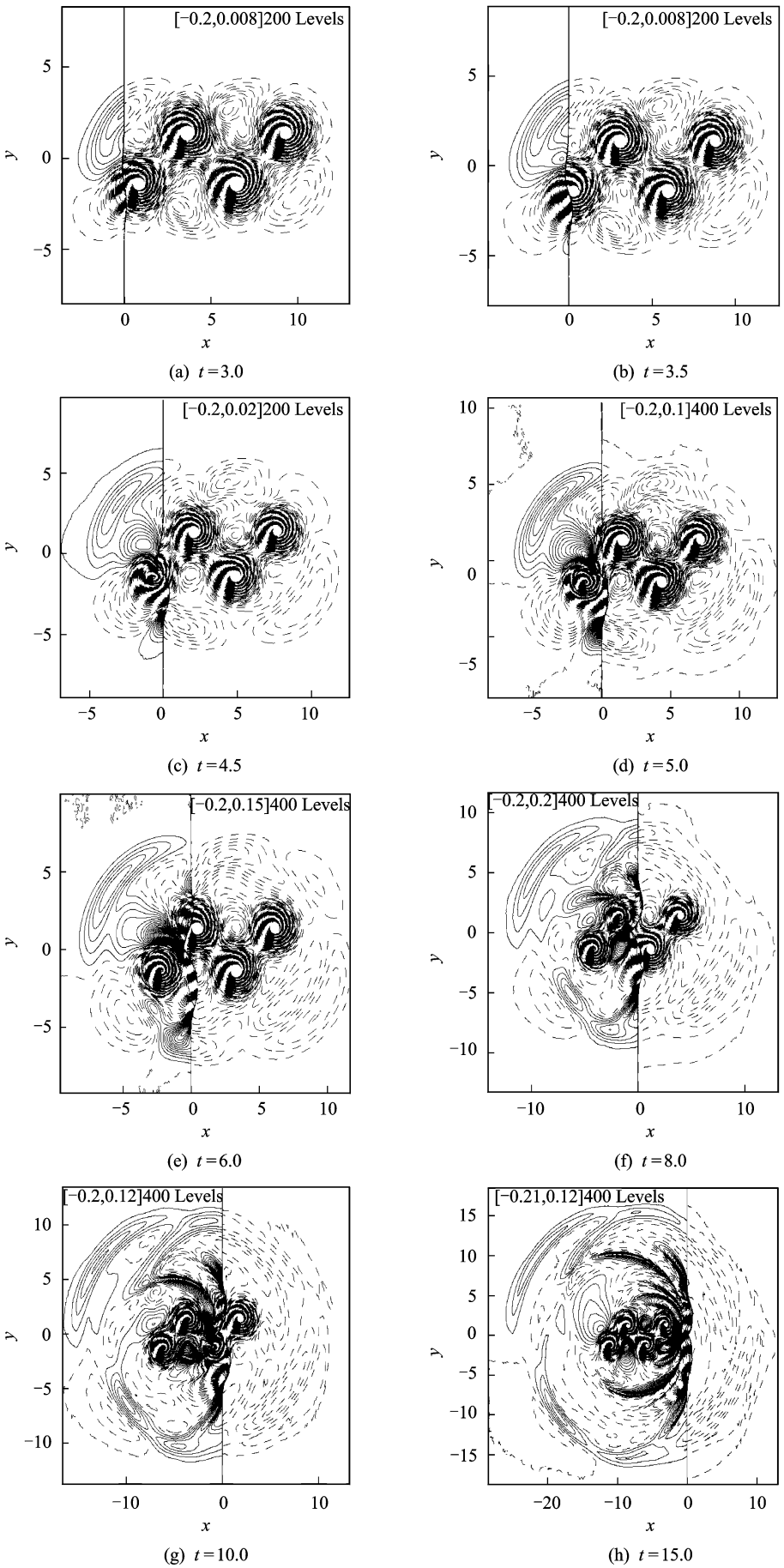

(a) $t=3.0$ (b) $t=3.5$

(c) $t=4.5$ (d) $t=5.0$

(e) $t=6.0$ (f) $t=8.0$

(g) $t=10.0$ (h) $t=15.0$

Fig. 5 Evolution of sound pressure of shock and vortex street composed of four vortices interaction($Ma_s=1.05$, $Ma_v=0.25$)

wave reforming(Figs. 5(g—h))

From Fig. 5, the vortex street traverses the shock wave. Owing to the break of the original sound wave and the reflected shock, the sound waves are irregular and chaotic. The merging is continuing, so we enlarge the computation region to ($-25 \leqslant x \leqslant 60$, $-35 \leqslant y \leqslant 35$). Fig. 6 is the picture of sound pressure iso-lines of $t = 30$. In Fig. 6 the compression region and the rarefaction region are arranged alternately. The breaking trace can be observed clearly, but it is difficult to distinguish the sound waves.

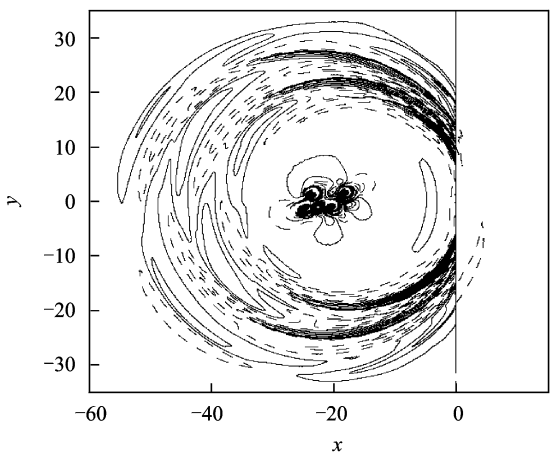

Fig. 6 Sound pressure of shock and vortex street interaction ($Ma_s = 1.05$, $Ma_v = 0.25$)

3 CONCLUSION

The phenomenon of shock focusing, folding, and crossing are much more clear and common. The reflected shock waves fold and reform a new strong shock which also interacts with the vortices. The shock focusing region interacts with the vortices and the vortex coupling proceeds meanwhile. The generated sound waves break down each other and merge constantly. The sound waves are also broken down by the reflected shocks. The study lays foundation for the future research of interactions between a shock and complex vortices in turbulence.

Acknowledgements

The authors acknowledge the help of Dr. Nan Gao.

References:

[1] Inoue O, Hattori Y. Sound generation by shock-vortex interactions[J]. J Fluid Mech, 1999,380(1):81-116.

[2] Zhang S H, Zhang Y T, Shu C W. Interaction of an oblique shock wave with a pair of parallel vortices: shock dynamics and mechanism of sound generation [J]. Physics of Fluids, 2006, 18(12): 126101-1-126101-21.

[3] Zhang Y T, Shu C W. Multistage interaction of a shock wave and a strong vortex[J]. Physics of Fluids, 2005,17(11):116101-1-116101-13.

[4] Shu C W. Essentially non-oscillatory and weighted essentially non-oscillatory scheme for hyperbolic conservation laws [R]. NASA/CR-97-206253 ICASE Report, 1997.

(Executive editor: Zhang Bei)